Electronic Supplementary Material (ESI) for ChemComm.
This journal is © The Royal Society of Chemistry 2023

Supporting Information

UV-induced Self-Reinforced Hydrogel Based on *In-situ* Hydrophobic Aggregation of Strained 1,2-Dithiolane Rings

Huiqing Zhong, Qinwen Tan, Dezhi Zhan, Aolin Wang, Yu Jiang,* and Daohong Zhang*

Key Laboratory of Catalysis and Energy Materials Chemistry of Ministry of Education & Hubei Key Laboratory of Catalysis and Materials Science, Hubei R&D Center of Hyperbranched Polymers Synthesis and Applications, South-Central Minzu University, Wuhan 430074, China.

Experimental Section

Materials

Methacrylic anhydride, lipoic acid, triethanolamine (TEA), 1,4-butanediol (BDO)1,8-octanediol, 4-dimethylaminopyridine (DMAP), N-(3-Dimethylaminopropyl)-N'-ethylcarbodiimide hydrochloride (EDCI), sodium chloride (NaCl), sodium sulfate (Na_2SO_4), 2-hydroxyethyl methacrylate (HEMA), and poly (ethylene glycol) methyl ether acrylate (PEGA, ~480 g/mol) and 2,2-Azobis(2-methylpropionitrile) (AIBN) were purchased from Aldrich and used as received. HEMA and PEGA were passed a column of basic aluminum oxide to remove the inhibitor. *N*, *N*-dimethylformamide (DMF), dichloromethane (DCM), petroleum ether (PE), ethyl acetate (EA) and chloroform ($CHCl_3$) were directly used. Tetrahydrofuran (THF) was refluxed over sodium/benzophenone and distilled under a nitrogen atmosphere just before use.

Characterization

The Fourier-transform infrared spectroscopy (FTIR) measurements were recorded on a spectrometer (Bruker Vertex 70, Germany). ^{1}H NMR and ^{13}C NMR were recorded on a spectrometer (Bruker Avance III 400 MHz, Germany) with $CDCl_3$ and DMSO-d_6 as solvent and TMS as internal standard. The size exclusion chromatography (SEC) measurements were recorded on a spectrometer (Waters 1515) using N, N-dimethylformamide (DMF) as the eluent with a flow rate of 0.3 mL/min at 35 ℃. The system was calibrated with linear polystyrene standards. The stress-strain curves of the hydrogel (length 25 mm × width 3 mm × thickness 0.3 mm) were recorded at room temperature using the tensile testing machine (Instron 5943, Instron, Norwood, MA, USA), using a 10 N load cell and loading rate of 10mm min^{-1} according to ASTM D638-14. All the samples were measured for at least three times, the tensile properties were denoted by average values with standard deviation. Error bars of the machanical property data represent the standard deviation of the mean (N = 3). UV-vis absorption spectra were recorded by Agilent Cary 5000 UV-Vis-NIR spectrophotometer using a standard quartz cuvette (10 mm) or thin-film quartz cell. The structures of the hydrogel

were recorded Raman spectroscopy (Thermo Fisher Scientific DXR2xi) with a laser wavelength of 532nm. The self-healing process of hydrogel was observed by optical microscopy (Nikon ECLIPSE Ni). Wide-angle X-ray diffraction (WAXD) patterns were collected on a Bruker AXS D8 ADVANCE X-ray diffractometer with Cu Kα radiation (λ = 1.5418 Å). The diffraction data were collected in the range of 2θ = 10-60° with a scan step size of 1° min^{-1}. Rheological behaviors of hydrogels were measured with an DHR-1 rheometer (TA Instruments, USA) equipped with either a 25 mm parallel plate fixture. The fracture surface morphologies of hydrogels were observed by scanning electron microscope on SU8010 (SEM, Japan Hitachi) at an acceleration of 2 KV.

Calculations

Swelling ratio (SR, %) was performed by immersing the sample (around 100.00mg) in deionized water (100ml) at room temperature, 60 °C for 12h. The swelling ratio was calculated according to the following equation

$$SR(\%) = (m_b - m_a)/m_a \times 100\%$$

Where m_a is the initial mass of the samples, and m_b is the mass after swelling.

The sample was photographed with an optical microscope at the fracture before and after healing. The formula for calculating the self-healing efficiency of rubber is expressed as

$$Self-healing\ efficiency = \left[\sigma_{(healed)}/\sigma_{(original)}\right] \times 100\%$$

Where $\sigma_{(original)}$ and $\sigma_{(healed)}$ are the tensile strength before and after healing, respectively.

Synthesis of 4-Hydroxybutyl methacrylate

Methacrylic anhydride (8.40 ml, 55.48 mmol) was slow added dropwise to a cooled solution of 1, 4-butanediol (5.00 ml, 55.48 mmol) and TEA (7.70 ml, 55.48 mmol) in chloroform (50.00 ml). The reaction was stirred at room temperature for 48 h, extracted with DCM and dried with sodium sulfate, and evaporated to an oil which was

chromatographed on silica gel using hexanes/ethyl acetate (4:1) to give 3.89 g (44% yield) of clear oil.

^{1}H NMR (400 MHz, $CDCl_3$) δ 6.04 (s, 1H), 5.50 (s, 1H), 4.12 (t, *J* = 6.4 Hz, 2H), 3.61 (t, *J* = 6.4 Hz, 2H), 2.80 (s, 1H), 1.88 (s, 3H), 1.84 - 1.72 (m, 2H), 1.72 - 1.59 (m, 2H). ^{13}C NMR (100 MHz, $CDCl_3$) δ 167.6, 136.3, 125.4, 64.5, 62.0, 29.0, 25.0, 18.2.

Synthesis of 8-Hydroxyoctyl methacrylate

Methacrylic anhydride (5.20 ml, 34.20 mmol) was slow added dropwise to a cooled solution of 1,8-Octanediol (5.00 g, 34.20 mmol) and TEA (4.70 ml, 34.20 mmol) in DMF (50.00 ml). The reaction was stirred at 60 ℃ overnight, extract with EA and dried with sodium sulfate, and evaporated to an oil which was chromatographed on silica gel using hexanes/ethyl acetate (4:1) to give 3.0 g (41% yield) of clear oil.

^{1}H NMR (400 MHz, $CDCl_3$) δ 6.10 (s, 1H), 5.55 (s, 1H), 4.06 (t, *J* = 6.7 Hz, 2H), 3.54 (t, *J* = 6.7 Hz, 2H), 2.51 (s, 1H), 1.87 (s, 3H), 1.64 - 1.56 (m, 2H), 1.52 - 1.45 (m, 2H), 1.34 (s, 8H). ^{13}C NMR (100 MHz, $CDCl_3$) δ 167.6, 136.4, 125.2, 64.7, 62.6, 32.6, 29.2, 29.1, 28.5, 25.8, 25.6, 18.2.

Synthesis of HEMA-C_nD

In a typical procedure for the synthesis process, HEMA-C_2D was prepared by the literature[1] as shown in **Scheme S1**. Briefly, a solution of lipoic acid (2.0 g, 9.7 mmol) and 2-hydroxyethyl methacrylate (1.20 ml, 9.7 mmol) in a mixture of DCM (30 mL) and the DMAP (0.6 g, 4.8 mmol) and EDCI (2.79 g, 14.5 mmol) was added as solids and stirred at 0 ℃ for 30 min and then stirred overnight at room temperature. After washing with 1M HCl (30 ml × 3), $NaHCO_3$ (30 ml × 3), and brine, the organic layer and dried over Na_2SO_4, and evaporated at reduced pressure to give the crude product. The residue was without further purified by column chromatography to afford 96% yield of HEMA-C_2D (2.96 g) as light-yellow oil. Other monomers were synthesized with a similar process.

^{1}H NMR (400 MHz, $CDCl_3$): δ 6.03 (s, 1H), 5.51 (s, 1H), 4.24 (s, 4H), 3.50 - 3.34 (m, 1H), 3.12 - 2.98 (m, 2H), 2.32 - 2.41 (m, 1H), 2.26 (m, 2H), 1.85 (s, 3H), 1.28-1.82 (m,

7H). ^{13}C NMR (100 MHz, $CDCl_3$): δ 173.1, 167.0, 135.8, 126.0, 62.4, 61.9, 56.2, 40.1, 38.4, 34.5, 33.8, 28.6, 24.5, 18.2.

HEMA-C_4D

^{1}H NMR (400 MHz, $CDCl_3$) δ 6.02 (s, 1H), 5.49 (s, 1H), 4.05 (m, 2H), 4.12 (m, 2H), 3.54 - 3.46 (m, 1H), 3.14 - 3.00 (m, 2H), 2.43 - 2.35 (m, 1H), 2.25 (m, 2H), 1.87 (s, 3H), 1.85 – 1.79 (m, 1H), 1.46 - 1.73 (m, 2H). ^{13}C NMR (100 MHz, $CDCl_3$) δ 173.4, 167.3, 136.3, 125.4, 64.1, 63.8, 56.3, 40.2, 38.5, 34.6, 34.0, 28.7, 25.3, 25.3, 24.6, 18.3.

HEMA-C_8D

^{1}H NMR (400 MHz, $CDCl_3$) δ 5.98 (s, 1H), 5.44 (s, 1H), 3.89 (m, 2H), 4.09 (m, 2H), 3.50 - 3.38 (m, 1H), 3.10 - 2.95 (m, 2H), 2.40 - 2.30 (m, 1H), 2.23 - 2.17 (m, 2H), 1.83 (s, 3H), 1.80 - 1.75 (m, 1H), 1.63 - 1.18 (m, 18H). ^{13}C NMR (100 MHz, $CDCl_3$) δ 173.5, 167.4, 136.4, 125.1, 64.6, 64.3, 56.3, 40.2, 38.5, 34.6, 34.0, 29.1, 29.1 28.7, 28.5, 28.5, 25.8, 25.8, 24.7, 18.3.

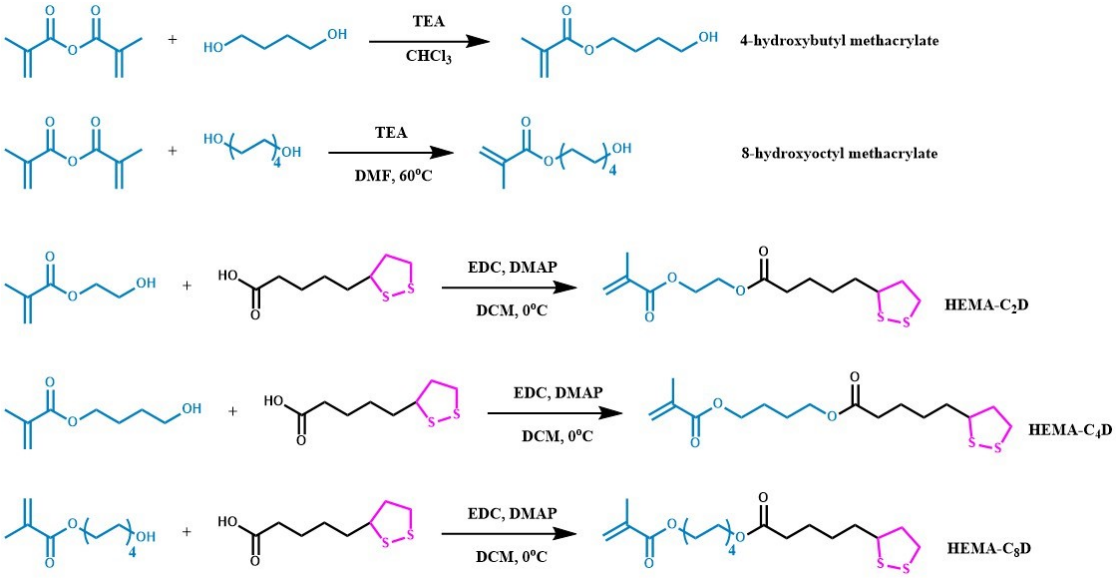

Scheme S1. Synthesis of 4-hydroxybutyl methacrylate, 8-hydroxyoctyl methacrylate, HEMA-C_2D, HEMA-C_4D, and HEMA-C_8D.

Synthesis of polymer PHEMA-xC_nD (Scheme S2)

In a typical procedure for the synthesis process, PHEMA-0.2C_4D was synthesized by free radical copolymerization of HEMA (0.63 g) and HEMA-C_4D (2.0 g), 1 mol %

azobisisobutyronitrile (AIBN) (0.01 g) in 150 ml THF. The mixture was degassed by three freeze-pump-thaw cycles. The polymerization was carried out at 60 ℃ for 24 h under an argon atmosphere. The obtained product was precipitated twice into ethyl acetate to remove the unreacted monomer and impurities and then was dried in *vacuo* at room temperature to yield PHEMA-0.2C_4D as yellow solid. Other copolymers with different compositions were synthesized by a similar process.

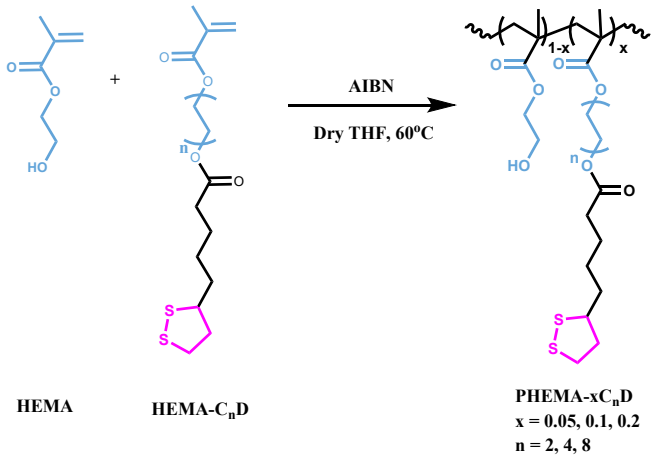

Scheme S2. Synthesis of polymer PHEMA-xC_nD.

Synthesis of polymer PHEMA-*co*-PPGEA-0.1C_2D (Scheme S3)

Step 1: PHEMA-*co*-PPGEA was synthesized by free radical copolymerization of HEMA (5.26 g) and PEGA (3.87 g) in 50 ml THF and 1 mol % of AIBN (0.08 g) was used as an initiator. The mixture was degassed by three freeze-pump-thaw cycles. The polymerization was carried out at 60 °C for 24 h under an argon atmosphere. The obtained product was precipitated twice into petroleum to remove the unreacted monomer and impurities and then was dried in *vacuo* at room temperature to yield PHEMA-*co*-PPGEA as a white solid. The molar ratio of the two monomers in the copolymer was 1:0.2.

Step 2: Lipoic acid (0.17 g), copolymer PHEMA-*co*-PPEGA (5.00 g), and DMAP (0.05 g) were added into a 100 mL flask. Then 50 mL THF was injected into the flask. The mixture was cooled to 0 °C, and EDCI (0.24 g) was added. Subsequently, the mixture was stirred at rt for 24 h. After the desired time, the reaction mixture was

precipitated twice into ethyl acetate to remove the unreacted monomer and impurities and then was dried in *vacuo* at room temperature to yield PHEMA-*co*-PPGEA-0.1C_2D as a yellow solid.

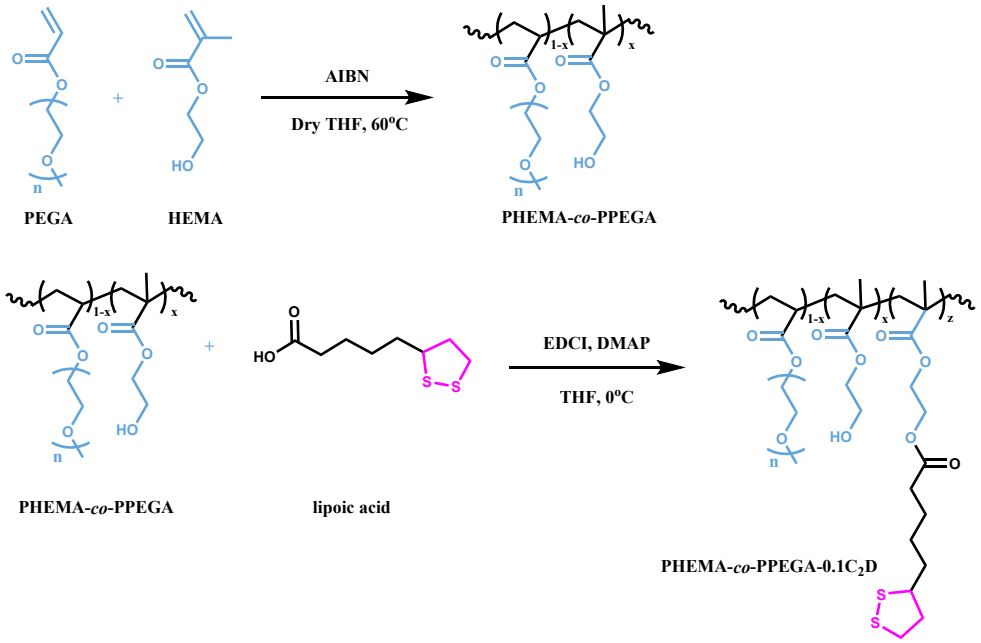

Scheme S3. Synthesis of polymer PHEMA-*co*-PPEGA-0.1C_2D.

Preparation of hydrogel film

In a typical process, the copolymer PHEMA-0.2C_4D was dissolved in DMF to form a homogeneous solution with a concentration of 200 mg/mL. Then, the PHEMA-0.2C_4D solution was poured into a horizontally placed PTFE mold. After the solvent gradually evaporated at 60 ℃, the sample was immersed in a large amount of deionized water to obtain hydrogel film. The film was peeled from the PTFE after several hours; however, the swelling process was continued overnight to achieve equilibrium. Different amounts of polymer solution were added to the mold to give the hydrogel films with different thicknesses.

Characterization Data

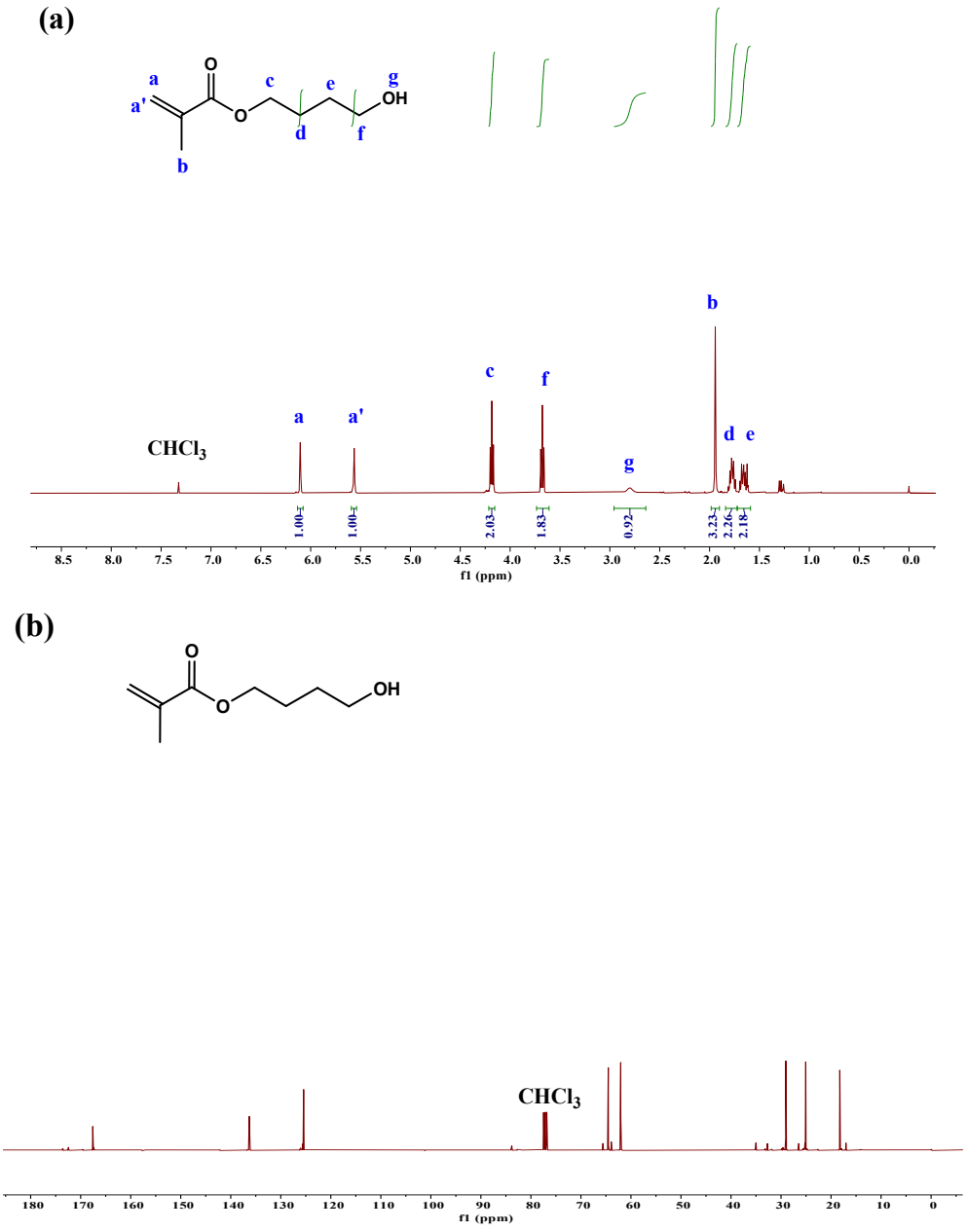

Figure S1. (a) ^{1}H NMR ($CDCl_3$, 400 MHz, 25 °C) and (b) ^{13}C NMR ($CDCl_3$, 100 MHz, 25 °C) spectra of 4-hydroxybutyl methacrylate.

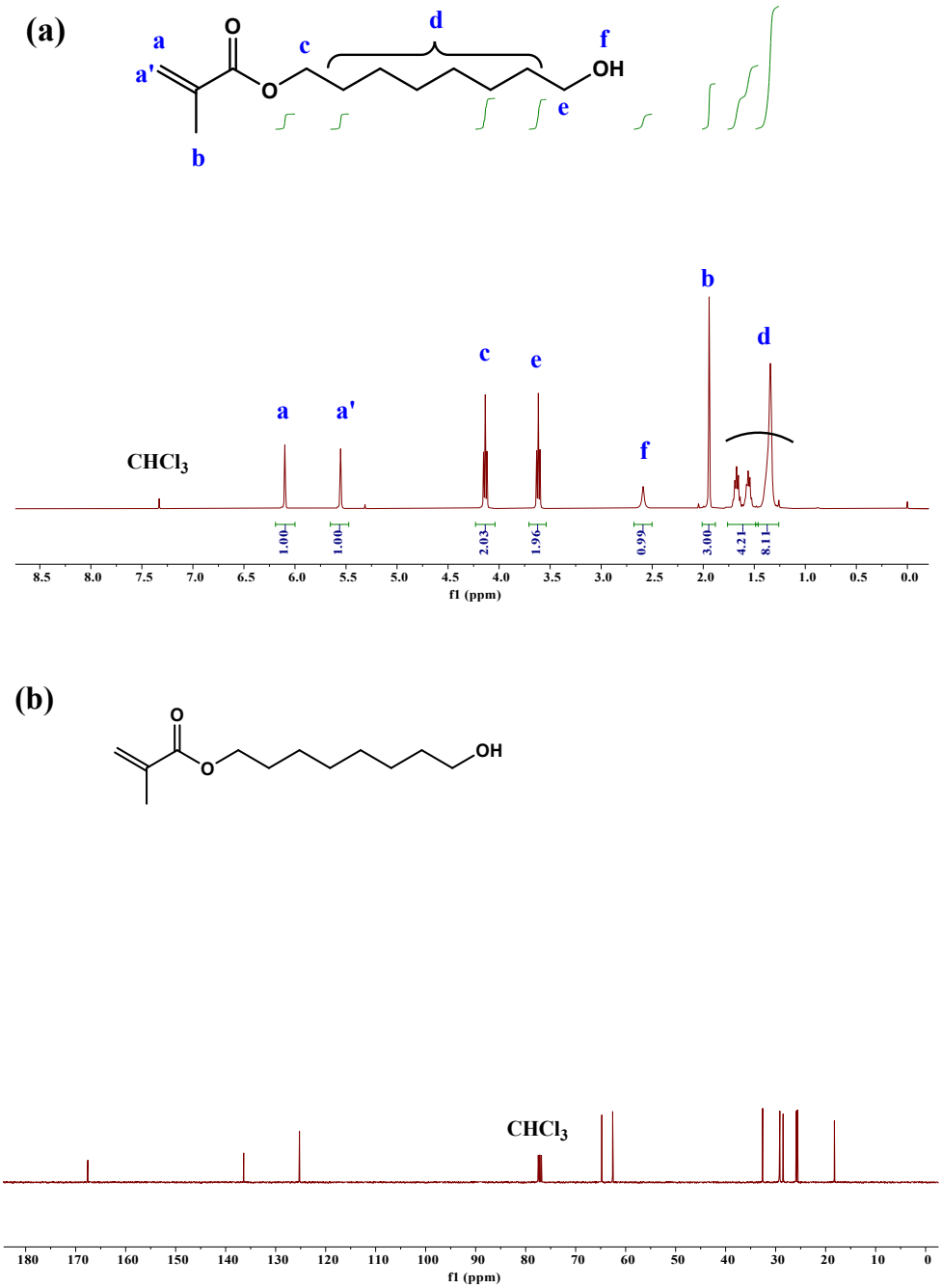

Figure S2. (a) ^{1}H NMR ($CDCl_3$, 400 MHz, 25 °C) and (b) ^{13}C NMR ($CDCl_3$, 100MHz, 25 °C) spectra of 8-hydroxyoctyl methacrylate.

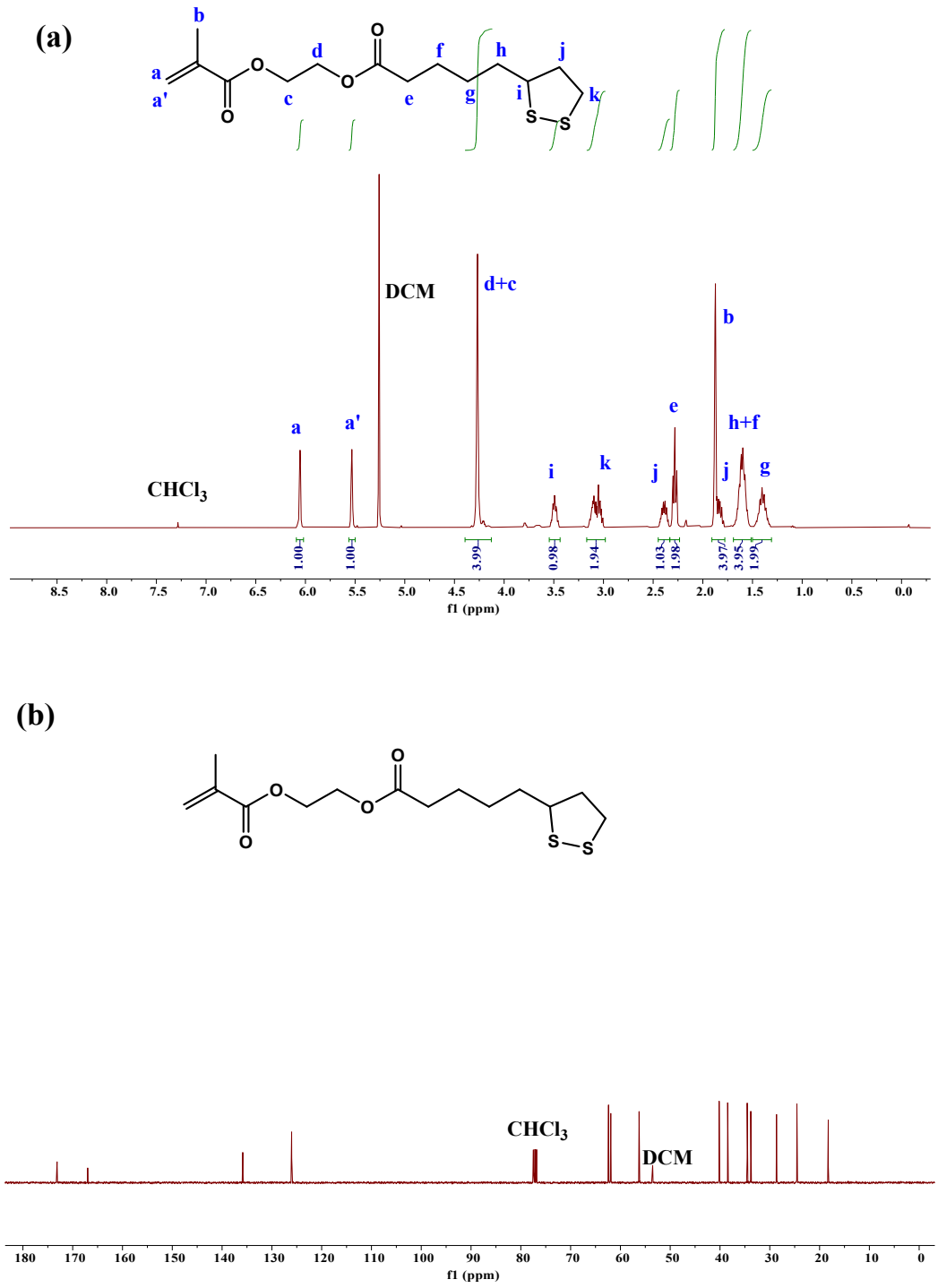

Figure S3. (a) ^{1}H NMR ($CDCl_3$, 400 MHz, 25 °C) and (b) ^{13}C NMR ($CDCl_3$, 100MHz, 25 °C) spectra of HEMA-C_2D.

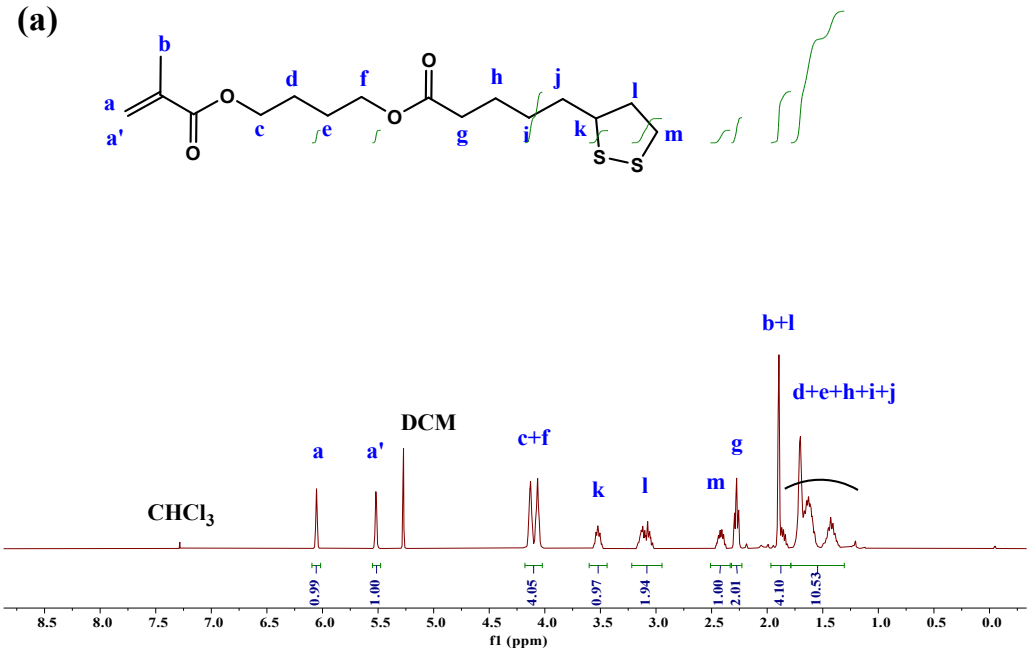

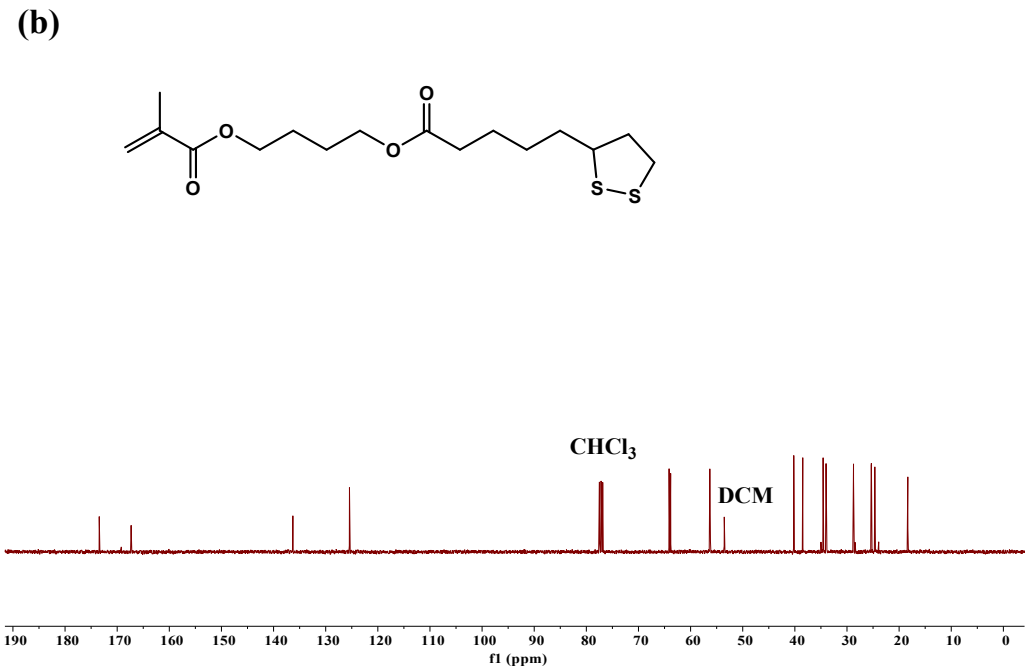

Figure S4. (a) ^{1}H NMR ($CDCl_3$, 400 MHz, 25 °C) and (b) ^{13}C NMR ($CDCl_3$, 100MHz, 25 °C) spectra of HEMA-C_4D.

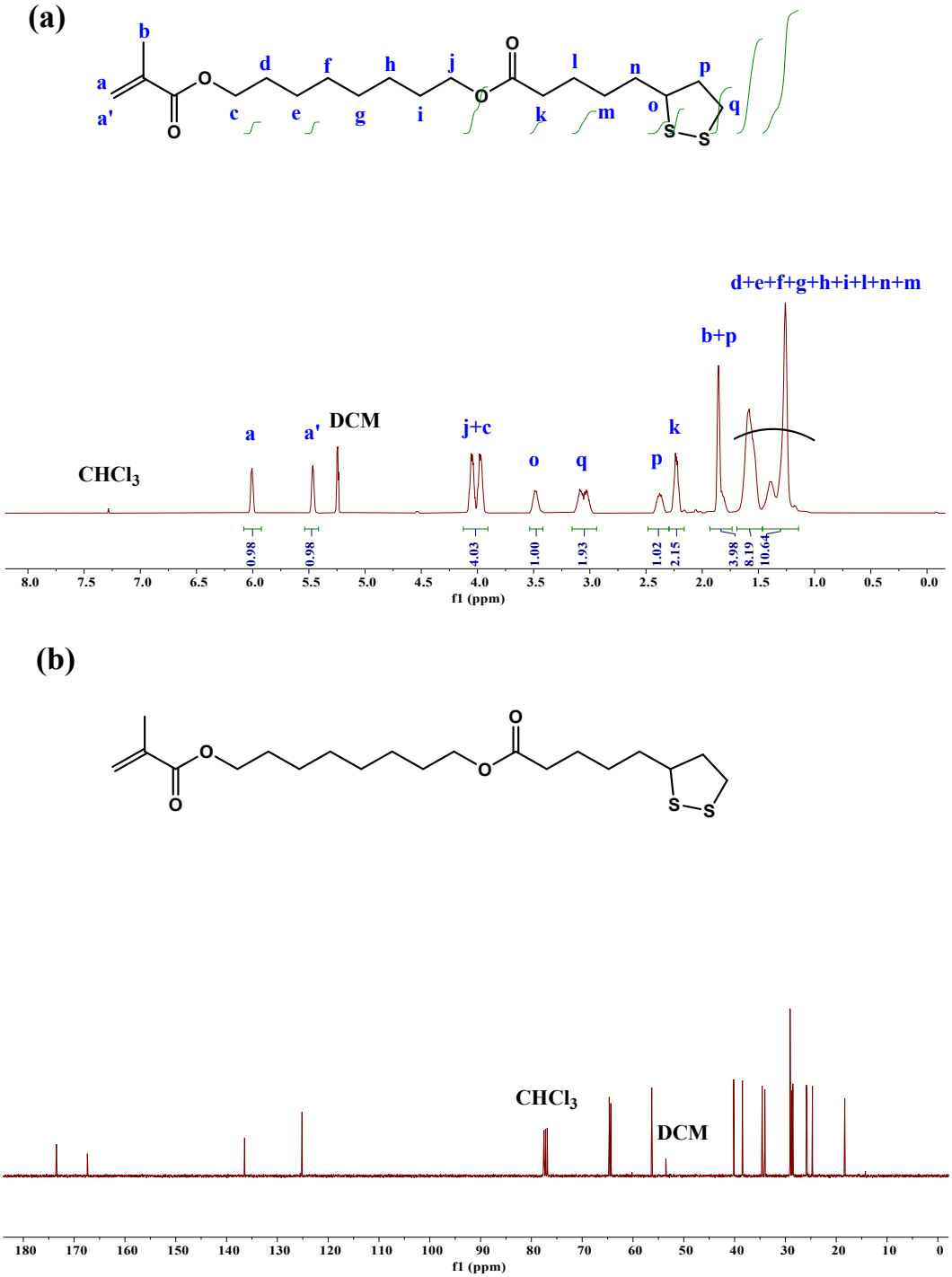

Figure S5. (a) ^{1}H NMR ($CDCl_3$, 400 MHz, 25 °C) and (b) ^{13}C NMR ($CDCl_3$, 100MHz, 25 °C) spectra of HEMA-C_8D.

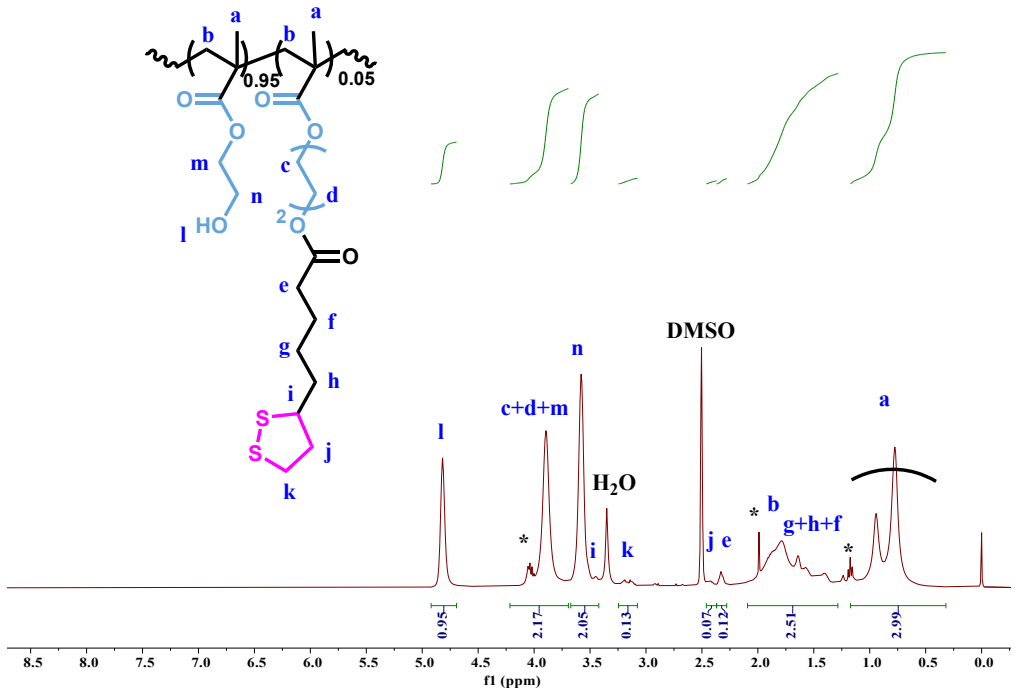

Figure S6. ^{1}H NMR (DMSO-d_6, 400 MHz, 25 °C) spectrum of PHEMA-0.05C_4D.

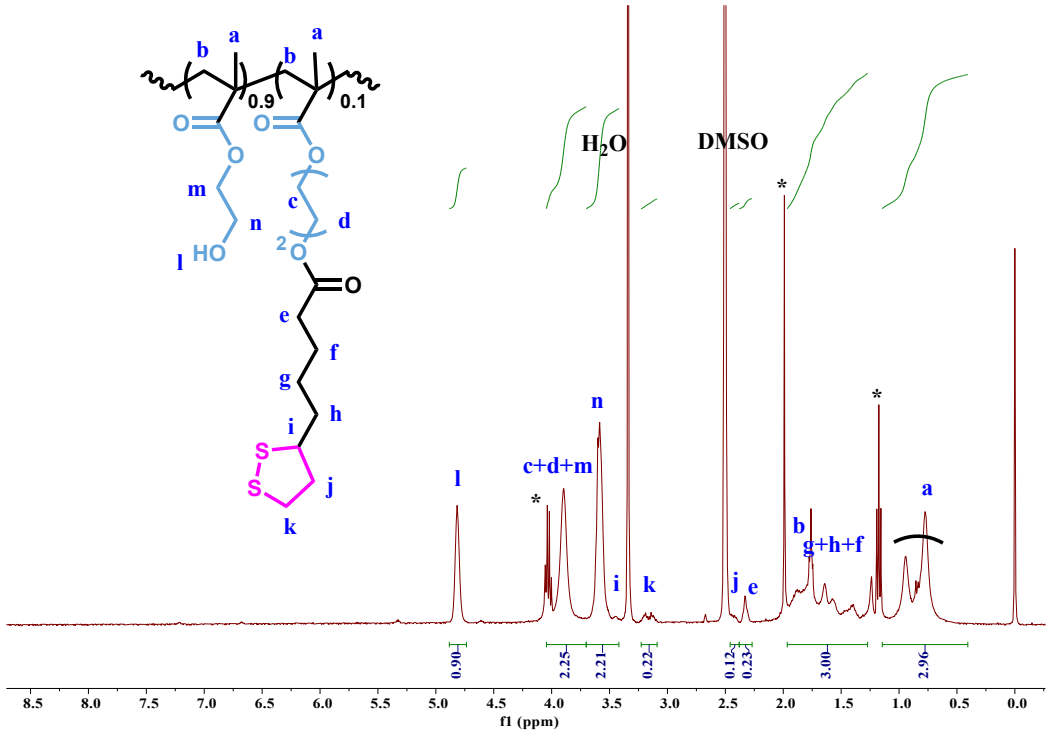

Figure S7. ^{1}H NMR (DMSO-d_6, 400 MHz, 25 °C) spectrum of PHEMA-0.1C_4D.

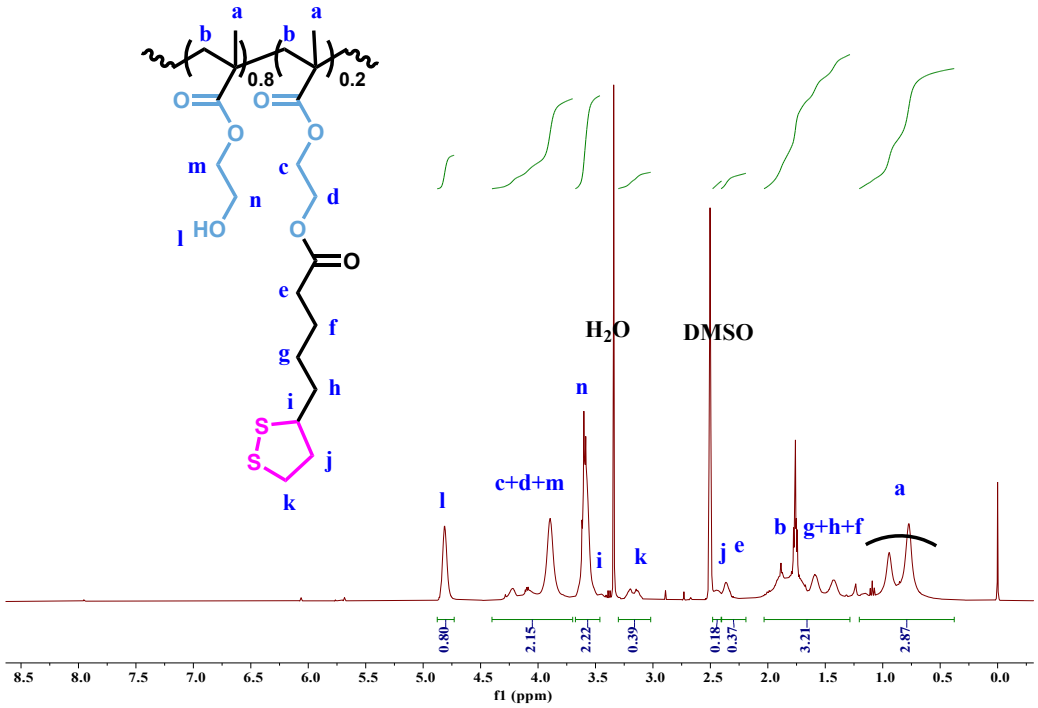

Figure S8. ^{1}H NMR (DMSO-d_6, 400 MHz, 25 °C) spectrum of PHEMA-0.2C_2D.

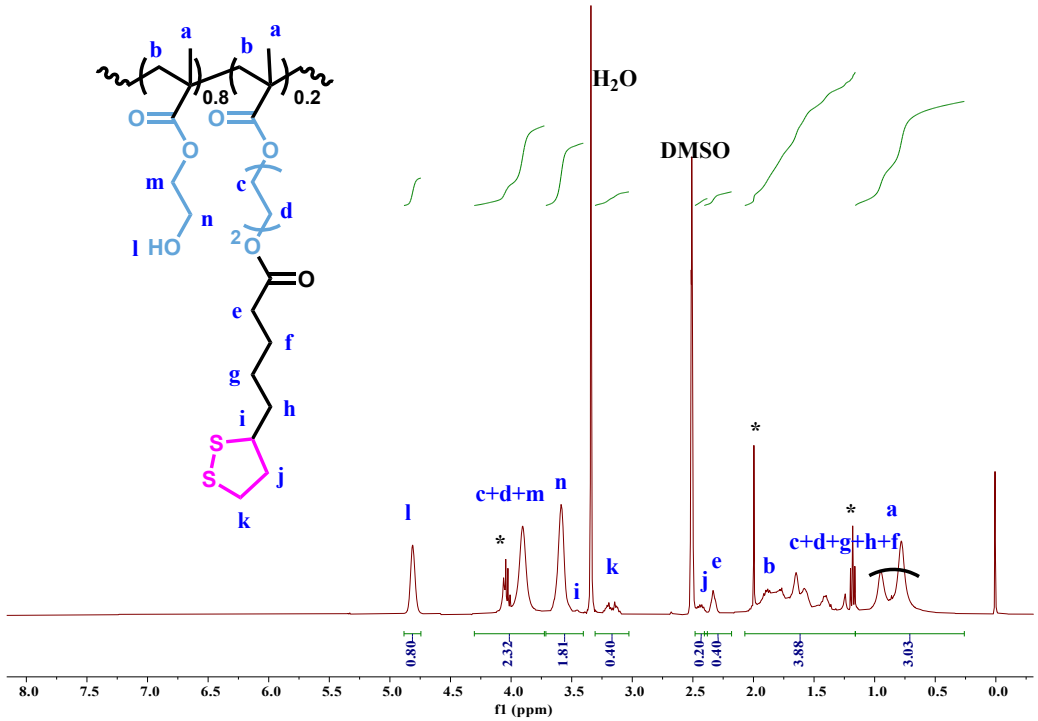

Figure S9. ^{1}H NMR (DMSO-d_6, 400 MHz, 25 °C) spectrum of PHEMA-0.2C_4D.

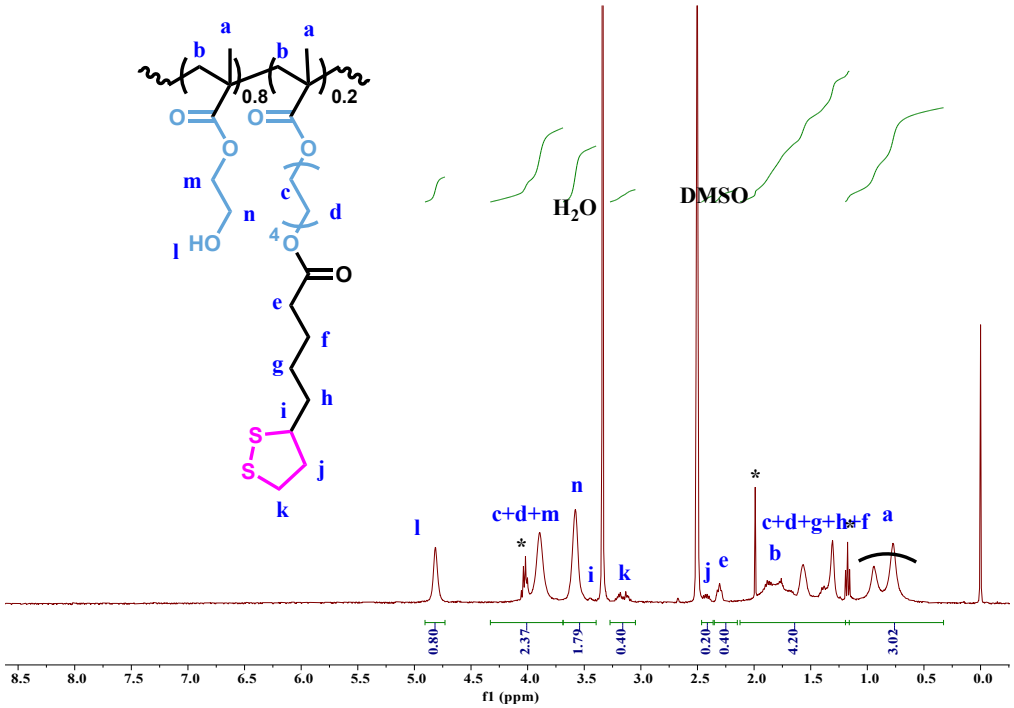

Figure S10. ^{1}H NMR (DMSO-d_6, 400 MHz, 25 °C) spectrum of PHEMA-0.2C_8D.

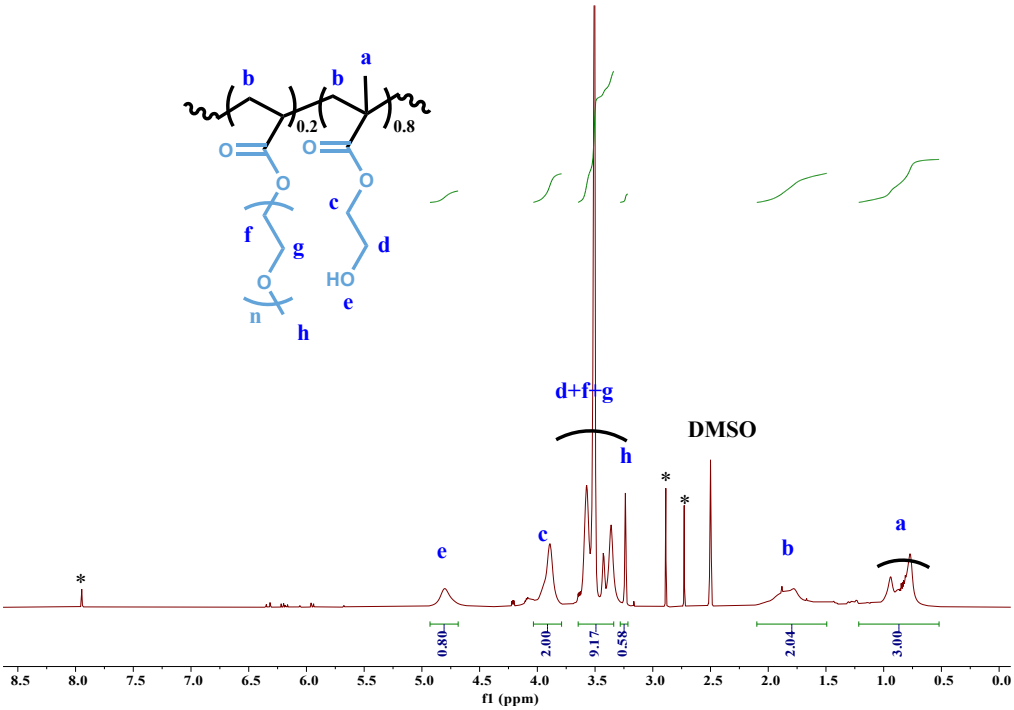

Figure S11. ^{1}H NMR (DMSO-d_6, 400 MHz, 25 °C) spectrum of PHEMA-*co*-PPEGA.

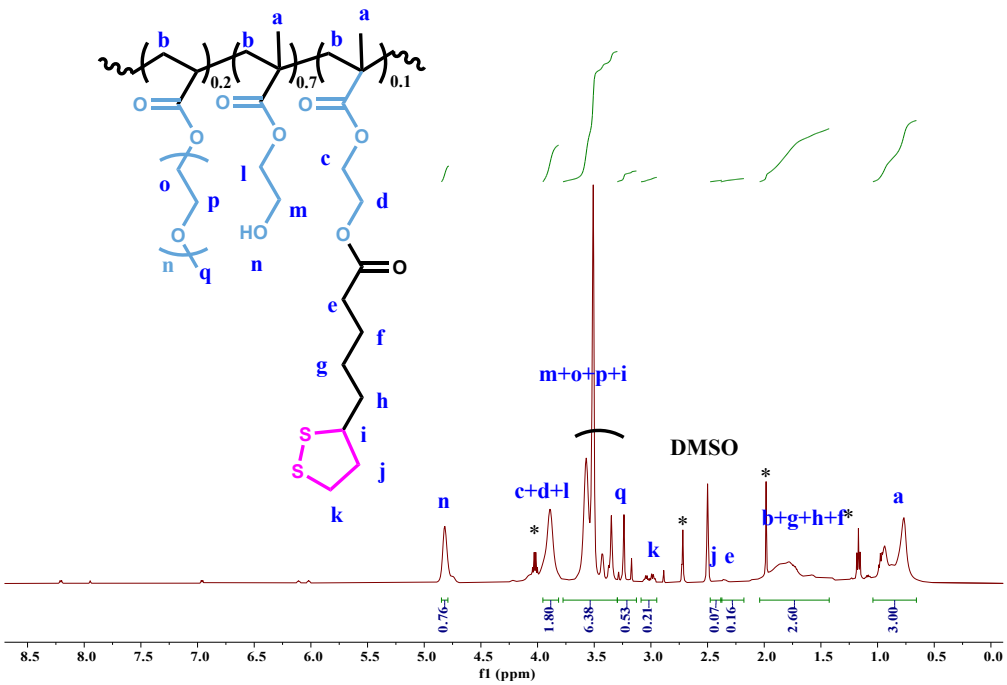

Figure S12. ^{1}H NMR (DMSO-d_6, 400 MHz, 25 °C) spectrum of PHEMA-*co*-PPEGA-0.1C_2D.

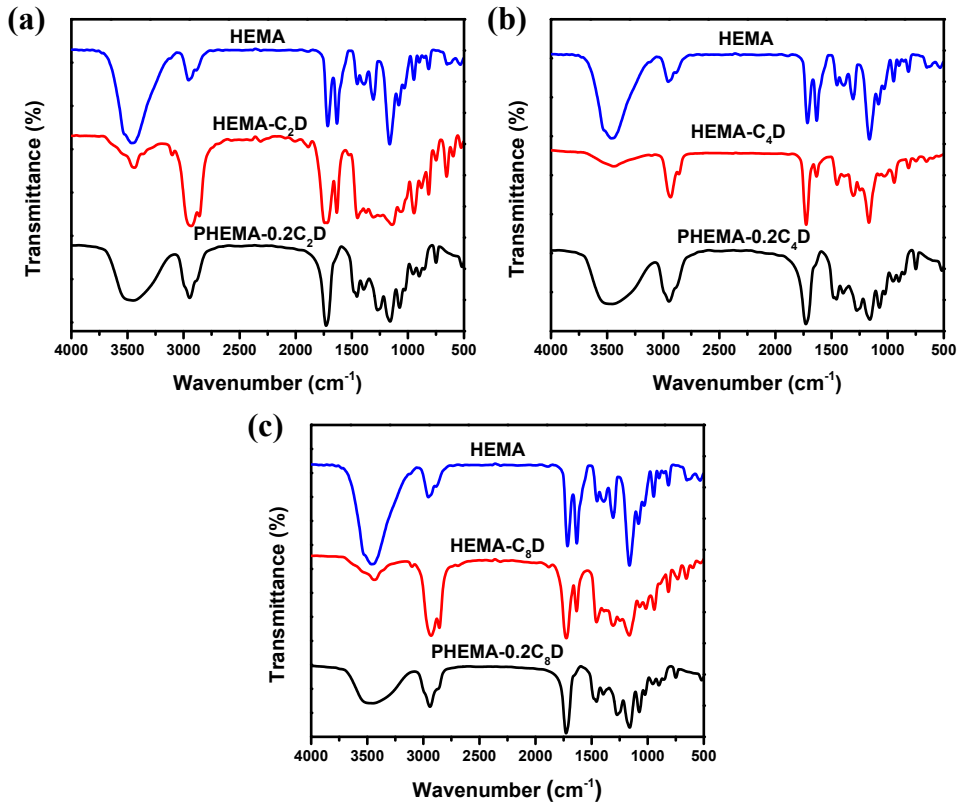

Figure S13. FT-IR spectra of (a) PHEMA-0.2C_2D, (b) PHEMA-0.2C_4D, and (c) PHEMA-0.2C_8D.

Table S1 Characteristics of the PHEMA-xC_nD polymers.

Sample	M_n (Da)[a]	PDI[a]
PHEMA-0.05C_4D	27000	1.23
PHEMA-0.1C_4D	26700	1.26
PHEMA-0.2C_4D	27000	1.23
PHEMA-0.2C_2D	27700	1.23
PHEMA-0.2C_8D	27000	1.29

[a] $M_{n,\,SEC}$ and PDI was determined by SEC (DMF, 25 ℃, PS standards).

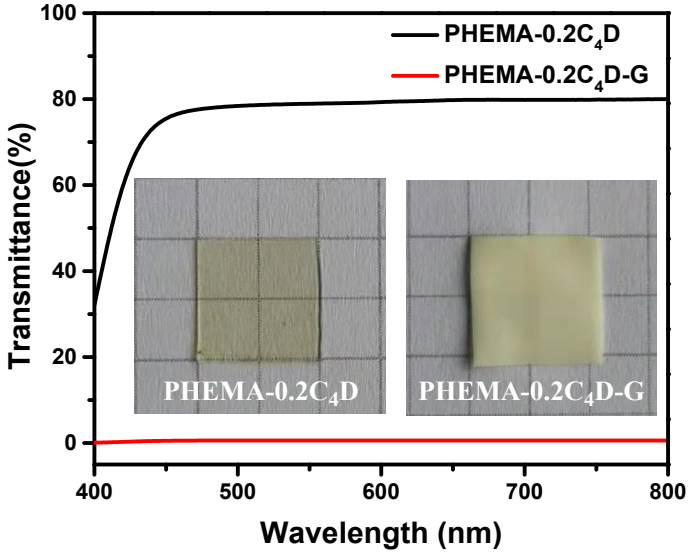

Figure S14. The transmission spectra of the PHEMA-0.2C_4D-G hydrogel before and after immersing in water with thickness of ~200 μm. (Insert: photographs showing the hydrogel before and after immersing in water)

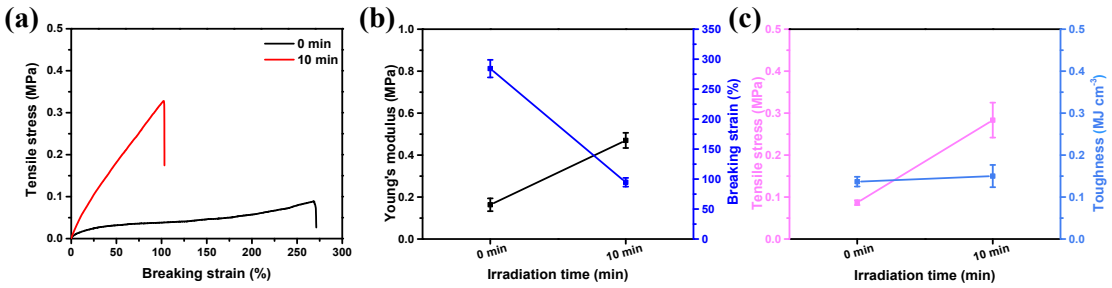

Figure S15. (a) Stress-strain curves of the PHMEA-0.05C_4D-G hydrogel with different UV irradiation time; (b-c) Young's modulus, breaking strain, tensile stress, and toughness of the PHMEA-0.05C_4D-G hydrogel with different UV irradiation time. Error bars represent the standard deviation of the mean (N = 3).

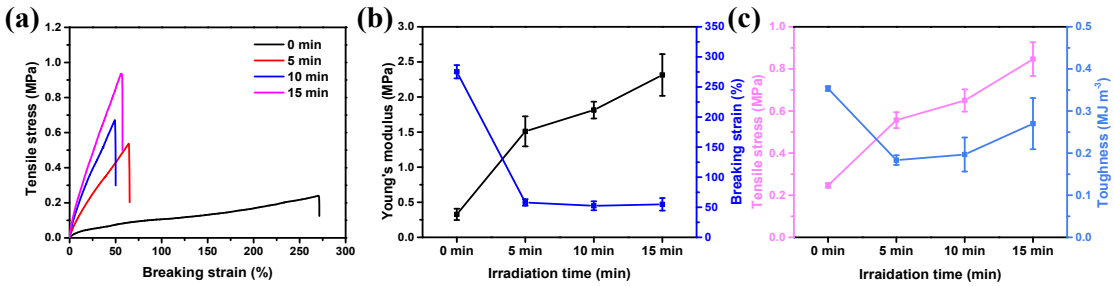

Figure S16. (a) Stress-strain curves of the PHMEA-0.1C_4D-G hydrogel with different UV irradiation time; (b-c) Young's modulus, breaking strain, tensile stress, and toughness of the PHMEA-0.1C_4D-G hydrogel with different UV irradiation time. Error bars represent the standard deviation of the mean (N = 3).

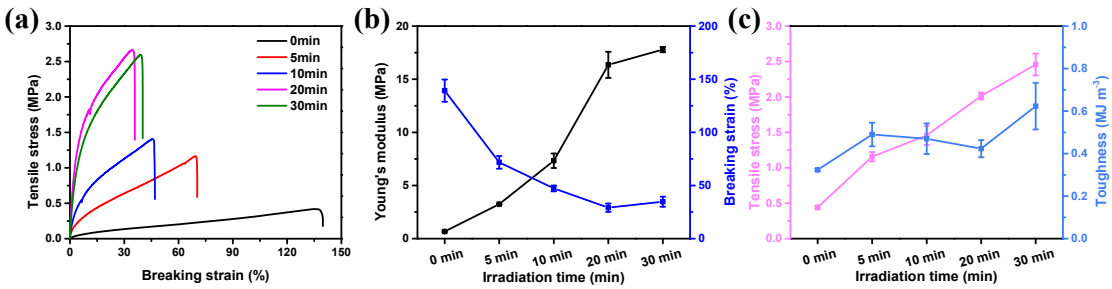

Figure S17. (a) Stress-strain curves of the PHMEA-0.2C_2D-G hydrogel with different UV irradiation time; (b-c) Young's modulus, breaking strain, tensile

stress, and toughness of the PHEMA-0.2C_2D-G hydrogel with different UV irradiation time. Error bars represent the standard deviation of the mean (N = 3).

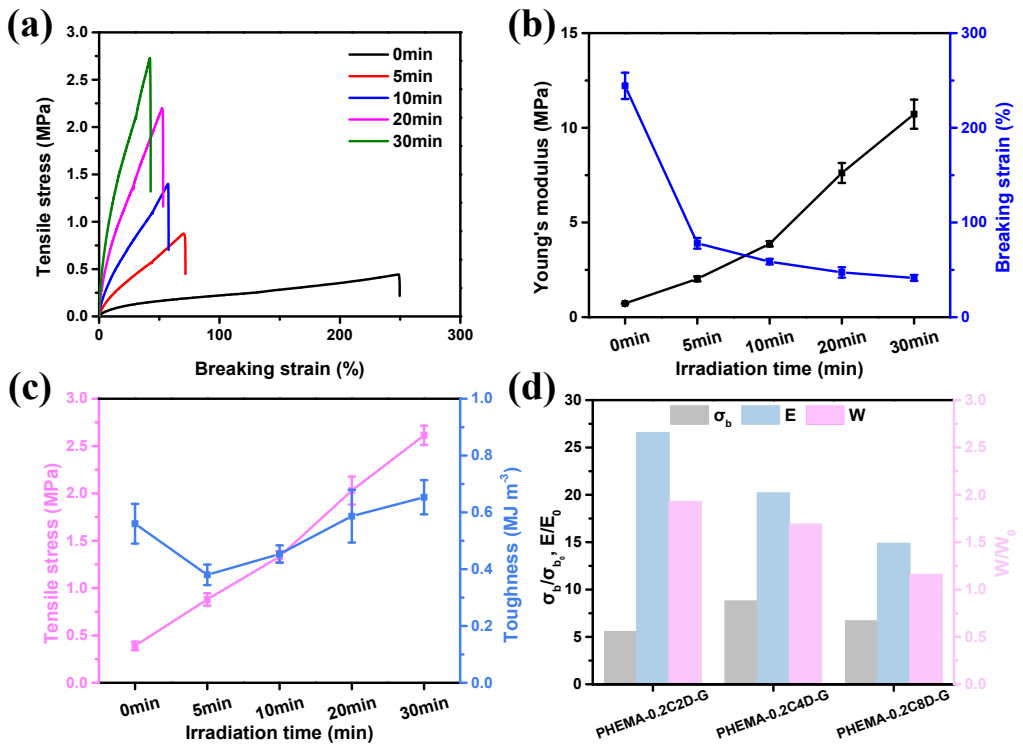

Figure S18. (a) Stress-strain curves of the PHMEA-0.2C_8D-G hydrogel with different UV irradiation time; (b-c) Young's modulus, breaking strain, tensile stress, and toughness of the PHEMA-0.2C_8D-G hydrogel with different UV irradiation time; (d) Compared enhancement of PHEMA-0.2C_nD-G hydrogel's Young's modulus (E/E_0), tensile stress (σ_b/σ_{b0}), and toughness (W/W_0). Error bars represent the standard deviation of the mean (N = 3).

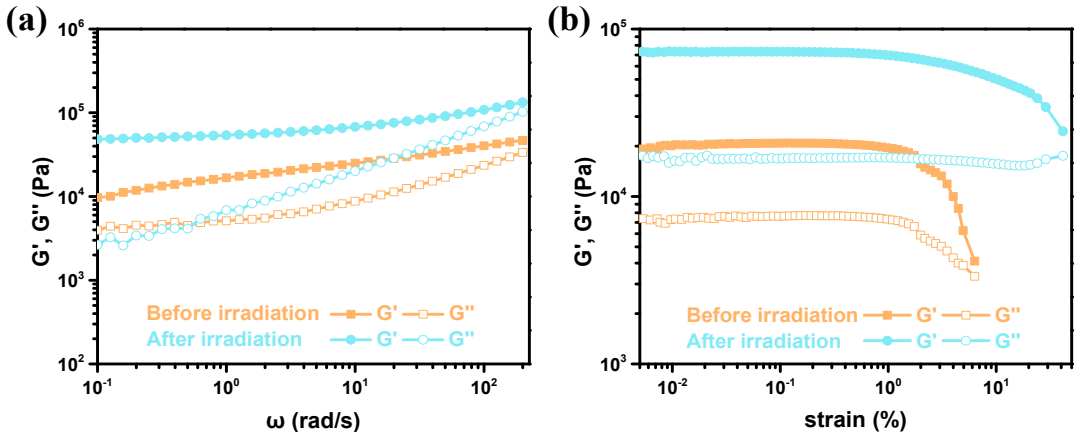

Figure S19. (a) Frequency sweep (at 0.1% strain) and (b) strain sweep (at 1 Hz frequency) of the PHEMA-0.05C_4D-G hydrogel before and after UV irradiation.

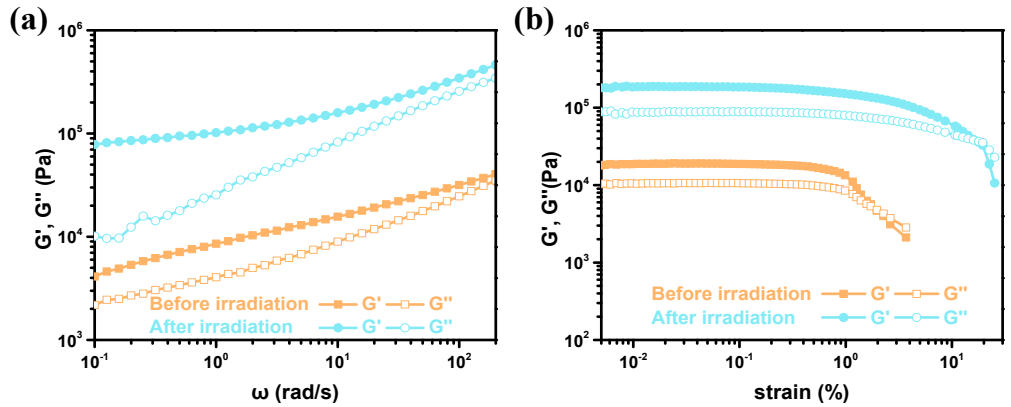

Figure S20. (a) Frequency sweep (at 0.1% strain) and (b) strain sweep (at 1 Hz frequency) of the PHEMA-0.1C_4D-G hydrogel before and after UV irradiation.

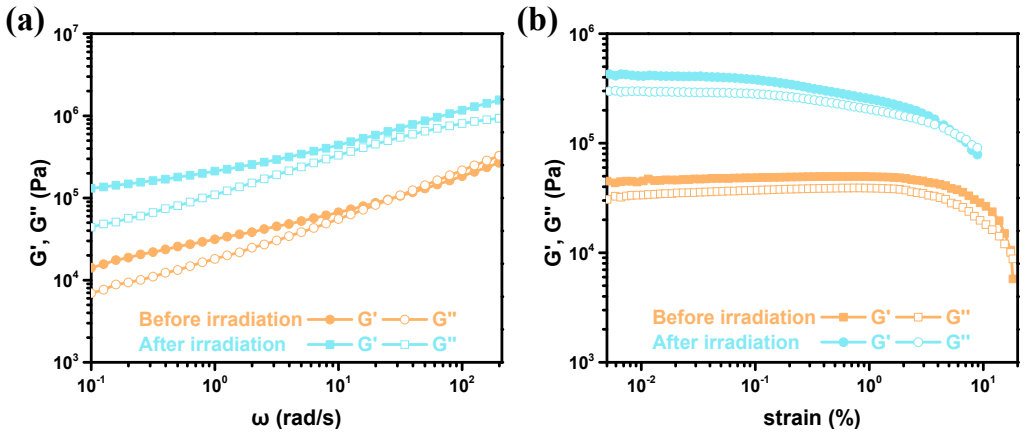

Figure S21. (a) Frequency sweep (at 0.1% strain) and (b) strain sweep (at 1 Hz frequency) of the PHEMA-0.2C_2D-G hydrogel before and after UV irradiation.

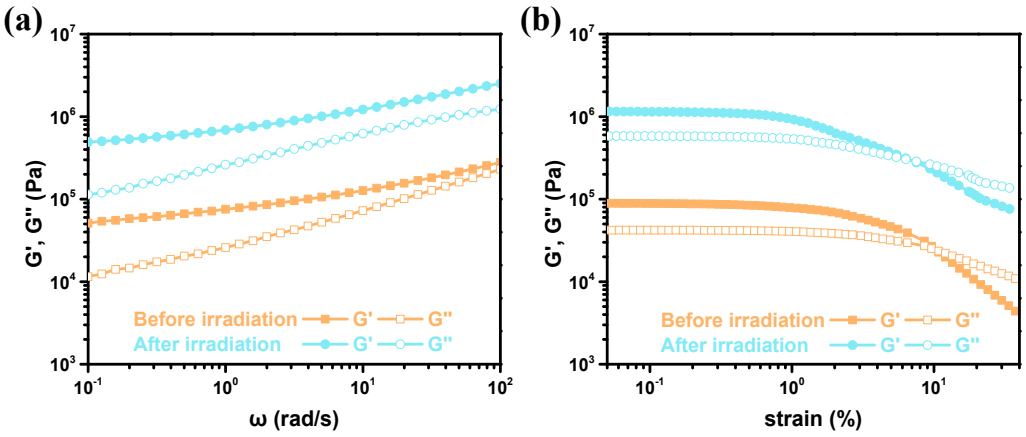

Figure S22. (a) Frequency sweep (at 0.1% strain) and (b) strain sweep (at 1 Hz frequency) of the PHEMA-0.2C_8D-G hydrogel before and after UV irradiation.

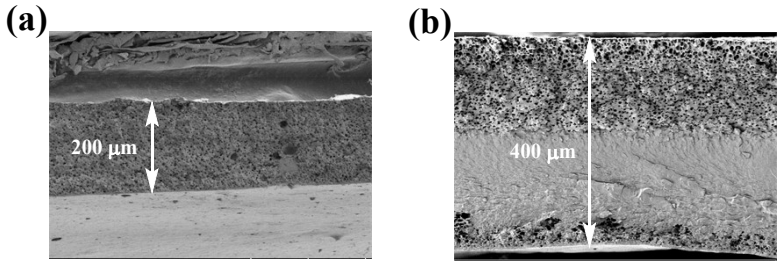

Figure S23. SEM micrograph of PHEMA-0.2C_4D-G hydrogel cross section with different thickness after 30 min UV irradiation. (a) 200 μm, (b) 400 μm. For the hydrogel with the thickness of 400 μm, the UV light cannot penetrate the hydrogel within 30 min irradiation and result in the asymmetric structure due to the short penetration property of UV light.

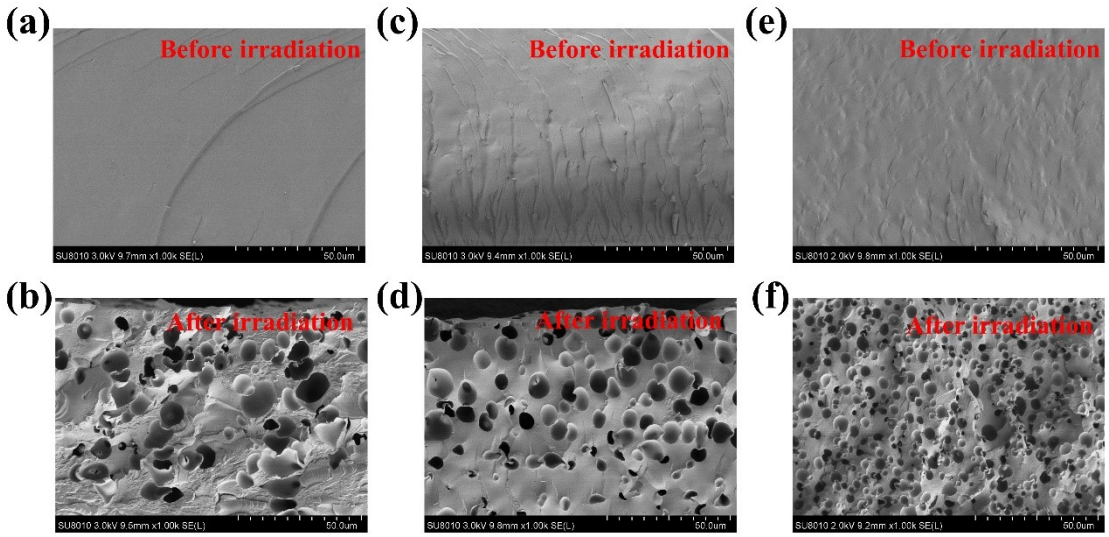

Figure S24. SEM micrographs of (a-b) PHEMA-0.05C_4D-G, (c-d) PHEMA-0.1C_4D-G, (e-f) PHEMA-0.2C_4D-G hydrogel cross sections before and after the UV irradiation.

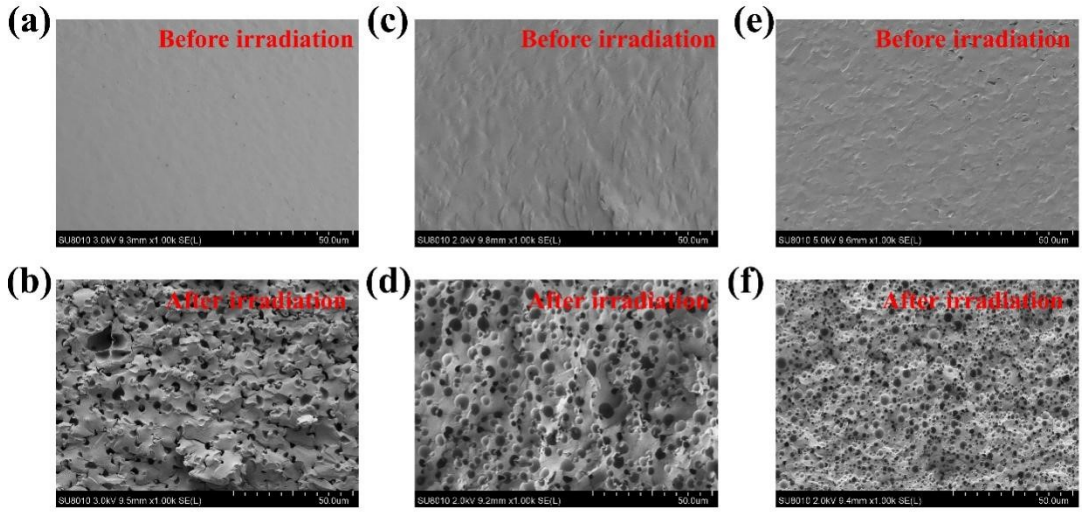

Figure S25. SEM micrographs of (a-b) PHEMA-0.2C_2D-G, (c-d) PHEMA-0.2C_4D-G, (e-f) PHEMA-0.2C_8D-G hydrogel cross sections before and after the UV irradiation.

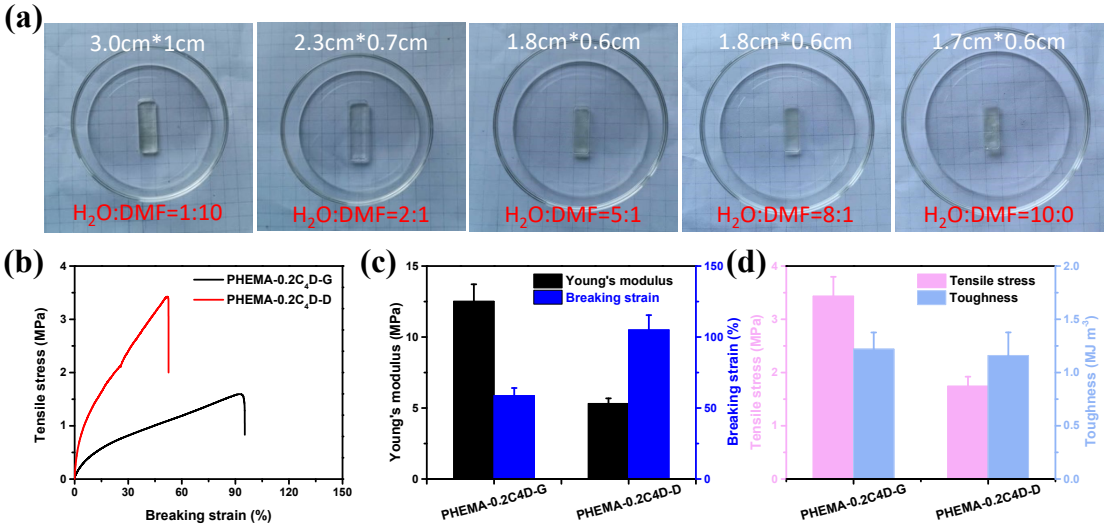

Figure S26. (a) Photographs showing the process of the solvent exchange for fabrication of PHEMA-0.2C_4D-D hydrogel; (b) Stress-strain curves of the PHMEA-0.2C_4D-G and PHEMA-0.2C_4D-D hydrogel; (c-d) Comparing Young's modulus, breaking strain, tensile stress, and toughness of the PHEMA-0.2C_4D-G and PHEMA-0.2C_4D-D hydrogel. Error bars represent the standard deviation of the mean (N = 3).

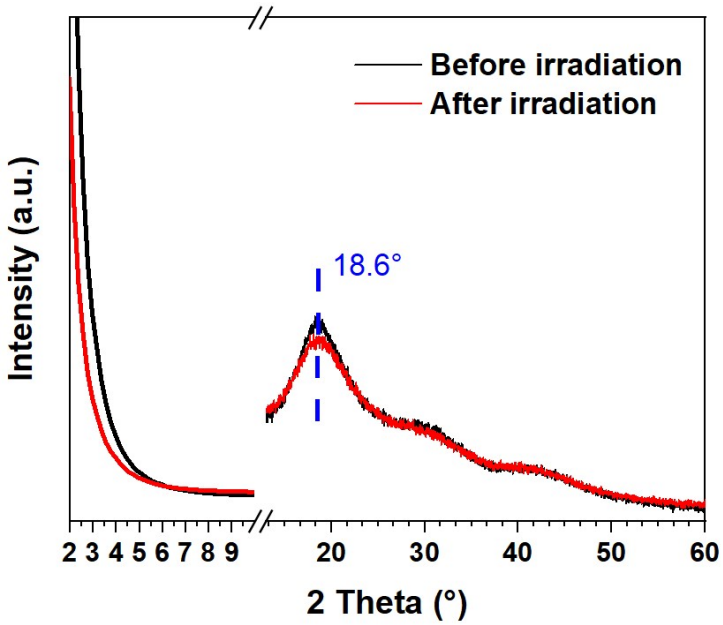

Figure S27. (a) XRD patterns for PHEMA-0.2C_4D-G hydrogel before and after UV irradiation.

The formation of hydrophobic domains in the original PHEMA-0.2C_4D-G hydrogel was further confirmed by X-ray diffraction (XRD) (black line in Figure S27). The hydrogels showed short-range order and the broad peak on the XRD pattern (high-angle, $2\theta = 18.6^{o}$) reflects the association of the hydrophobic side chains. As documented in the literature,[2-3] the position of this peak can reflect side-chain spacing d between alkyl side chains in the hydrophobic domains. According to the Bragg equation ($2d\sin\theta=0.154$ nm, where 0.154 nm is the wavelength of X-ray used for XRD collection), it can be calculated that d exhibited a small spacing with the value of 0.47 nm. On the other hand, there is no obvious peak at the low-angle area. All of these indicated that the nano-domains might employed as the crosslinking junctions in the hydrogels. The XRD pattern of the reinforced PHEMA-0.2C_4D-G hydrogel was almost the same as that of the original PHEMA-0.2C_4D-G hydrogel, indicating the hydrophobic aggregation state was rarely affected during the oligomerization process.

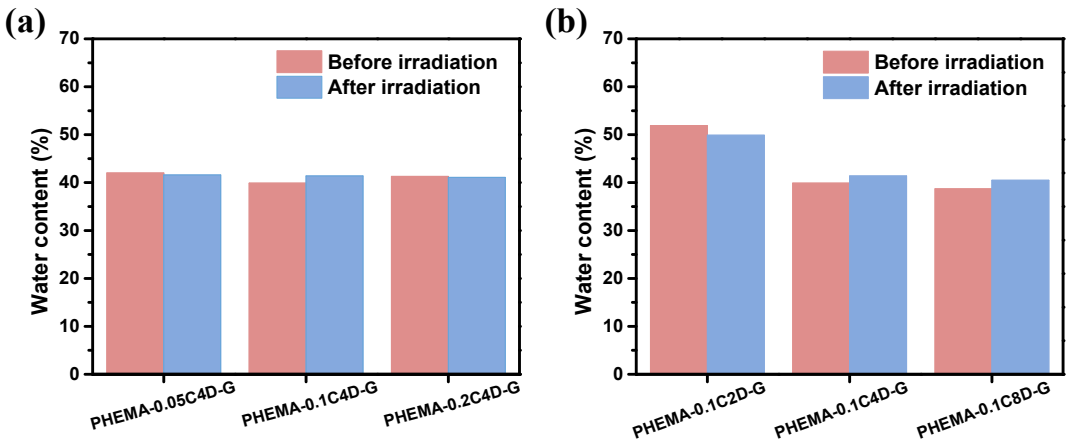

Figure S28. Water contents of the PHEMA-xC_nD-G hydrogels with (a) different contents of 1,2-dithiolane rings and (b) different spacer lengths before and after the UV irradiation.

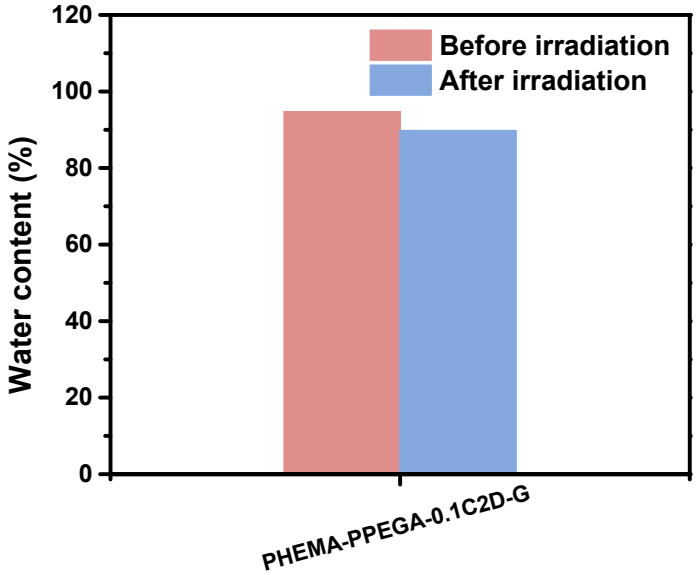

Figure S29. Water contents of PHEMA-*co*-PPEGA-0.1C_2D-G hydrogel before and after the UV irradiation.

Supplementary Reference

1 Y. H. Tran, M. J. Rasmuson, T. Emrick, J. Klier and S. R. Peyton, *Soft Matter*, 2017, **13**, 9007-9014.

2 J. Pan, L. Gao, W. Sun, S. Wang and X. Shi, *Macromolecules*, 2021, **54**, 5962-5973.

3 S. Wang, S. Li and L. Gao, *ACS Appl. Mater. Interfaces*, 2019, **11**, 43622-43630.